

# Hydrothermal Syntheses, Crystal Structures, and Photoluminescent Properties of Two Entangled Complexes with Rigid Bis(imidazolyl) Ligands

Yan Qi,<sup>[a]</sup> Yanhui Li,<sup>\*[a]</sup> and Yue Wang<sup>[b]</sup>

**Keywords:** Rigid bis(imidazole) ligand; Interpenetration; Polyrotaxane; Polycatenane; Topology

**Abstract.** Two new entangled complexes, namely, [Zn(bibp)(L<sup>1</sup>)] (**1**) and [Co(bib)(L<sup>2</sup>)]·H<sub>2</sub>O (**2**) [bibp = 4,4'-bis(1-imidazolyl)biphenyl, bib = 1,4-bis(1-imidazolyl)-benzene, H<sub>2</sub>L<sup>1</sup> = 4,4'-oxydibenzoic acid and H<sub>2</sub>L<sup>2</sup> = 4,4'-(2,2'-oxybis(ethane-2,1-diyl)bis(oxy))dibenzoic acid] were synthesized hydrothermally and characterized by IR spectroscopy, elemental analyses, and single crystal X-ray diffraction tech-

niques. Complex **1** presents a uninodal 4-connected **dmp** net with five-fold interpenetration containing left- and right-handed single-helical (ZnL<sup>1</sup>)<sub>n</sub> chains. Complex **2** displays both polyrotaxane and polycatenane characteristics. Furthermore, thermogravimetric studies of **1** and **2** and photoluminescent property of **1** were also investigated.

## Introduction

Particular attention has been recently devoted to entangled systems because of their undisputed beauty and potential applications as materials for gas storage, separation, and catalysis.<sup>[1,2]</sup> There are some comprehensive reviews by *Robson*, *Batten*, and *Ciani's* groups of many fascinating entangled structures, such as the common catenated arrays (for example, interpenetration) and the more complex rotaxane-like species, viz. polycatenated, polythreaded, and polyknotted species.<sup>[3–5]</sup> Conceptually, interpenetrating networks can be described as a number of individual nets participating in interpenetration with each other. However, polycatenation differs from interpenetration in that the whole catenated array has a higher dimensionality than that of the component motifs and that each individual motif is catenated only with the surrounding ones and not with all the others. To date, although some polycatenated coordination polymers have been reported by us and other groups,<sup>[6,7]</sup> the topological frameworks containing two kinds of entangled motifs in one compound are still quite rare. Only a few fascinating structures showing both polyrotaxane and polycatenane characters have been observed.<sup>[8]</sup> In addition, the exploration of coordination polymer with mixed ligands (esp. N-ligands and carboxylate ligands) continues to attract considerable interest.<sup>[9]</sup>

Taking inspiration from our previous work, our synthetic strategy is to select rigid bis(imidazole) ligand, namely, 4,4'-bis(1-imidazolyl)biphenyl (bibp) and 1,4-bis(1-imidazolyl)-benzene (bib) as organic linkers and the flexible dicarboxylic

acids, viz. 4,4'-oxydibenzoic acid (H<sub>2</sub>L<sup>1</sup>) and 4,4'-[2,2'-oxybis(ethane-2,1-diyl)bis(oxy)]dibenzoic acid (H<sub>2</sub>L<sup>2</sup>) as co-ligands, attributed to their diverse coordination modes and high structural stability.<sup>[9a,10]</sup> Fortunately, two novel entangled complexes [Zn(bibp)(L<sup>1</sup>)] (**1**) and [Co(bib)(L<sup>2</sup>)]·H<sub>2</sub>O (**2**) were successfully isolated. The syntheses, structures, thermal and photoluminescent studies in detail are listed below.

## Results and Discussion

### Structure Description

Single-crystal structure analysis reveals that complex **1** crystallizes in the orthorhombic space group *Pnna*. The asymmetric unit consists of one independent Zn<sup>II</sup> ion, one (L<sup>1</sup>)<sup>2-</sup> anion, and one bibp ligand. As shown in Figure 1a, the Zn<sup>II</sup> ion is coordinated by two (L<sup>1</sup>)<sup>2-</sup> oxygen atoms and two bibp nitrogen atoms to give the distorted ZnO<sub>2</sub>N<sub>2</sub> tetrahedral arrangement. The Zn–O bond length is 1.967(3) Å and the Zn–N bond length is 2.001(4) Å, both consistent with corresponding bond lengths found in the literature.<sup>[11]</sup>

The completely deprotonated (L<sup>1</sup>)<sup>2-</sup> ligands (in which the O3/O3' atoms are disordered) adopt *cis* conformation and connect the adjacent Zn<sup>II</sup> ions to form 1D left- and right-handed (ZnL<sup>1</sup>)<sub>n</sub> helical chains along *b* direction (Figure 1b) and the pitch of the helices is 22.199 Å. A width of helical tube is ca. 8.18 × 8.13 Å (the nearest distance between two opposite atoms in the tube). Each bibp ligand connects two neighboring central zinc atoms to give a zigzag chain. The overall 3D net is formed by the intersection, at the shared zinc nodes, of the 1D bibp chains and the 1D L<sup>1</sup> left- and right-handed helices. An analysis by using TOPOS<sup>[12]</sup> indicates that the coordination framework of **1** represents a uninodal 4-connected net with Schläfli symbol: (6<sup>5</sup>·8), the extended one being (6·6·6·6·6<sup>2</sup>·8<sup>5</sup>), assigned to the unusual **dmp** net according to Wells' classification (Figure 1c). The reported **dmp** nets are limited only ob-

\* Dr. Y. Li

Fax: +86-532-85953693

E-Mail: liyanhui@tsinghua.org.cn

[a] College of Electromechanical Engineering  
Qingdao University  
Qingdao city, P. R. China

[b] College of Chemistry and Environment  
Qingdao University  
Qingdao city, P. R. China

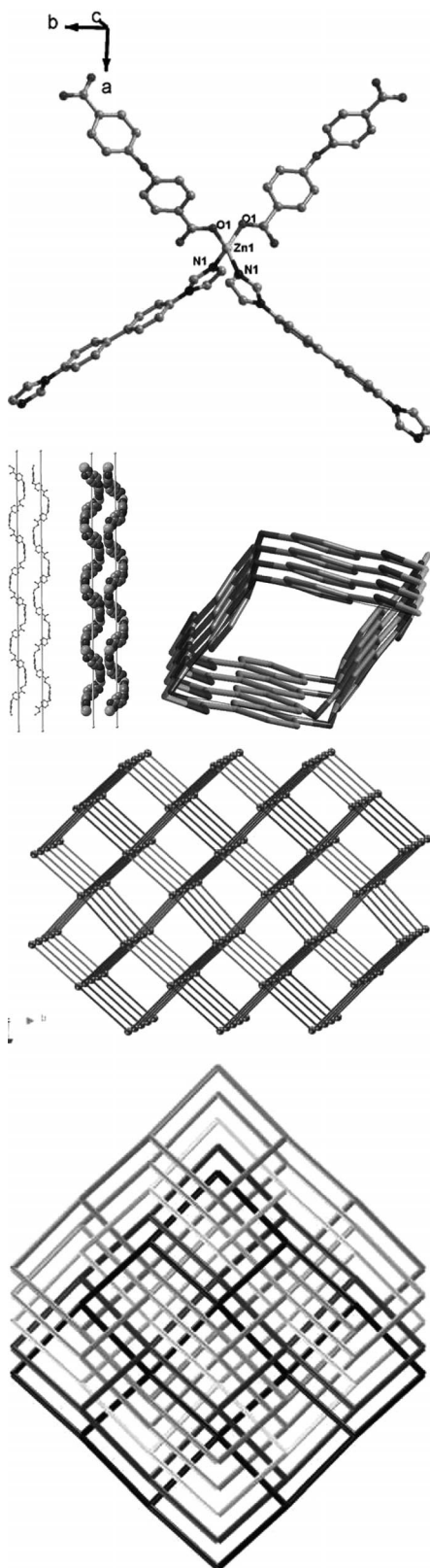


**Figure 1.** (a). Coordination around the  $\text{Zn}^{\text{II}}$  atom in **1**. All hydrogen atoms are omitted for clarity. (b) Perspective (left) and space-filling (middle) views of the 1D  $[\text{ZnL}]_n$  helical chain and the tubular motif shown by the helices, with the width being ca.  $8.18 \times 8.13 \text{ \AA}$  (right). (c) Schematic view of the 3D 4-connected **dmp** net in **1**. (d) The fivefold interpenetrating networks in **1**.

served in several compounds so far in the Reticular Chemistry Structure Resource (RCSR) database.<sup>[13]</sup> Interestingly, such five nets interpenetrate (Figure 1d). Also, it is noticeable that the structure of **1** is completely different from another zinc complex combined with the same mixed ligands, namely,  $[\text{Zn}_2(\text{obba})_2(\text{bimb})_2 \cdot (\text{DMF})_2 \cdot (\text{H}_2\text{O})_{3.5}]_n$  [ $\text{H}_2\text{obba}$  = 4,4'-oxydibenzoic acid;  $\text{bimb}$  = 4,4'-bis(1-imidazolyl)biphenyl], which exhibits a 3D chiral porous framework.<sup>[11]</sup>

Single crystal X-ray analysis reveals that complex **2** crystallizes in the triclinic space group  $P\bar{1}$ . The asymmetric unit consists of one independent  $\text{Co}^{\text{II}}$  ion, one  $(\text{L}^2)^{2-}$  anion, one bib ligand, and one free water molecule. As shown in Figure 2a, each cobalt atom is coordinated by two  $(\text{L}^2)^{2-}$  oxygen atoms and two bib nitrogen atoms to give a distorted  $\text{CoO}_2\text{N}_2$  tetrahedral arrangement. The Co–O/N bond lengths range from 1.9550(17) to 2.049(2)  $\text{\AA}$ , which are similar to those found in other related cobalt complexes.<sup>[14]</sup>

The completely deprotonated  $(\text{L}^2)^{2-}$  ligands also adopt *cis* conformation and connect the adjacent  $\text{Co}^{\text{II}}$  ions to form 40-membered  $\text{Co}_2(\text{L}^2)_2$  ring. Each bib ligand shows *trans* conformation with dihedral angle of two imidazole rings being  $27.19^\circ$ . The extension of the structure into a 1D ladder-like chain is accomplished by linear a pair of bib ligands linking the  $\text{Co}_2(\text{L}^2)_2$  loops, as shown in Figure 2b. That is to say, each cobalt atom is connected to three others: two via single bib bridges and a third by pairs of  $(\text{L}^2)^{2-}$  anions. Of particular interest, the most striking feature of complex **2** is that a pair of identical 1D single nets is interlocked with each other in a 1D  $\rightarrow$  2D parallel fashion thus directly leading to the formation of a 2D polycatenane-like structure containing rotaxane-like motifs (Figure 2c). As shown in Figure 2c, the  $\text{Co}_2(\text{L}^2)_2$  loops of each net are threaded by two Co–bib–Co rods of the other nets up and down, and vice versa. Therefore, the structure of **2** shows both polyrotaxane and polycatenane characteristics.

### Thermogravimetry

To study the thermal stability of **1** and **2**, thermogravimetric analysis (TGA) was performed on the single crystal samples of **1** and **2** in a nitrogen atmosphere with a heating rate of  $5^\circ\text{C}\cdot\text{min}^{-1}$  (Figure 3). Compound **2** lost the free water molecules at  $65\text{--}150^\circ\text{C}$  (obsd. 2.95%, calcd. 2.85%) and the frameworks of these compounds can be stable up to ca.  $240^\circ\text{C}$  for **1** and ca.  $260^\circ\text{C}$  for **2**. The resulting residue of compounds **1** and **2** remain as ZnO (calcd. 13.39%, found 14.72%) and CoO (calcd. 11.86%, found 11.65%), respectively, after the complete decomposition of the organic ligands.

### Photoluminescence

Photoluminescence experiments for **1** were performed at room temperature in the solid state. The emission bands for the free rigid bibp ligand is demonstrated at 355 nm and 373 nm ( $\lambda_{\text{ex}} = 280 \text{ nm}$ ) which can be assigned to the ligand-centered  $\pi \rightarrow \pi^*$  transitions of the benzene-imidazole rings.<sup>[15]</sup> Excitation of **1** at 330 nm produces one broad emission peak at 361 nm (Figure 4), probably be attributed to intraligand charge

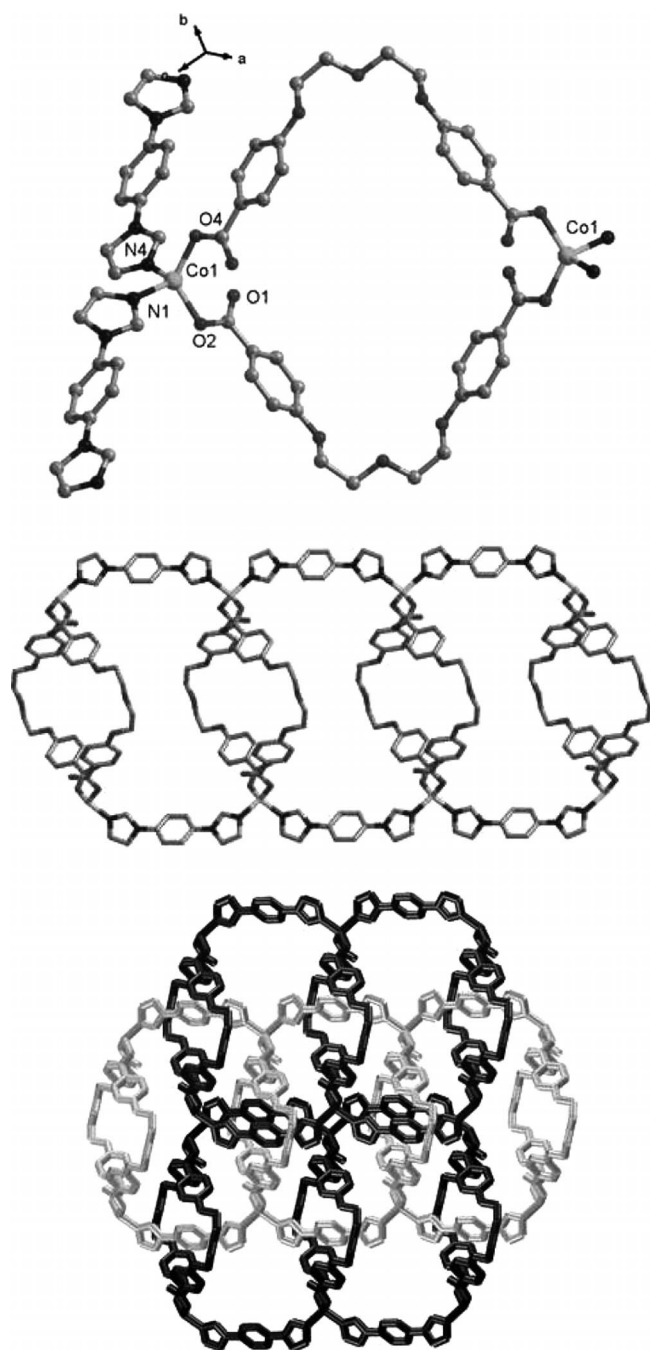


**Figure 2.** (a) Coordination around the  $\text{Co}^{\text{II}}$  atom in **2**. All hydrogen atoms and water molecules are omitted for clarity. (b). Perspective views of the 1D ladder-like chain containing  $\text{Co}_2(\text{L}^2)_2$  loops of **2**. (c) The schematic view of the polyrotaxane and polycatenane motifs in **2**.

transfer of the bibp ligand, because the  $\text{Zn}^{\text{II}}$  ion is difficult to oxidize or to reduce due to its  $d^{10}$  configuration.<sup>[9c,9d,10a]</sup>

## Conclusions

Two new 3D entangled coordination complexes were successfully isolated. Complex **1** presents a fivefold interpenetrated uninodal 4-connected **dmp** net. Complex **2** displays both polyrotaxane and polycatenane characteristics. In **1** and **2**

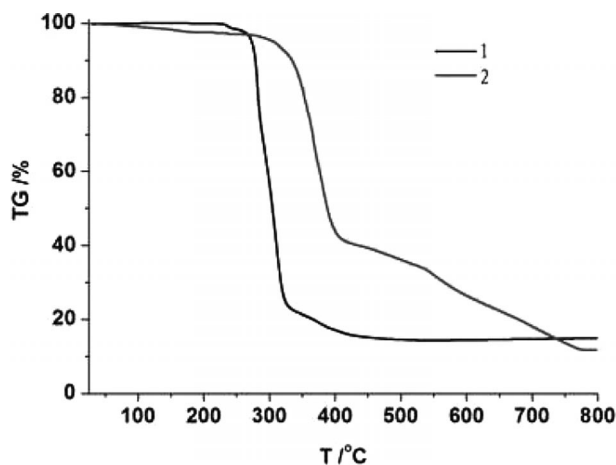


**Figure 3.** TG curve of compounds **1** and **2**.

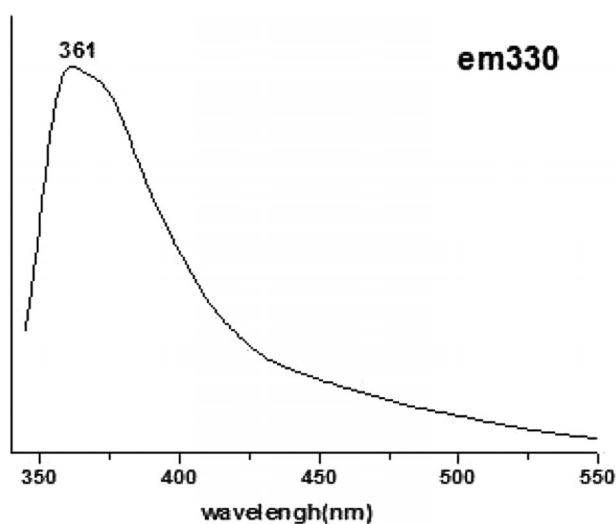


**Figure 4.** Solid-state emission spectra of **1** at room temperature.

flexible aromatic dicarboxylate anions, both adopting *cis* conformations, plays a key role on the ultimate frameworks. In **2** cobalt atoms are coordinated to  $(\text{L}^2)^{2-}$  anions to form  $\text{Co}_2(\text{L}^2)_2$  loops, while in **1** zinc ions are coordinated to aromatic dicarboxylate anions to form a pair of 1D left- and right-handed  $(\text{ZnL}^1)_n$  helical chains. As expected, compound **1** displays photoluminescence property.

## Experimental Section

**Materials and General Procedures:** Solvents and all the ligands (bib, bibp,  $\text{H}_2\text{L}^1$ , and  $\text{H}_2\text{L}^2$ ) for synthesis were purchased commercially and used as received. C, H and N analyses were performed with a Perkin-Elmer 240 analyzer. The IR spectrum was recorded as KBr pellets with a Nicolet Magna-FT-IR 560 spectrometer in the 4000–400  $\text{cm}^{-1}$  region. The photoluminescence measurements were carried out on crystalline samples at room temperature, and the spectra were collected with a Hitachi F-2500FL spectrophotometer. The thermogravimetric analyses were investigated with a standard TG analyzer in a nitrogen flow at a heating rate of 5  $^\circ\text{C}\cdot\text{min}^{-1}$  for all measurements.

**Synthesis of 1:** A mixture of  $\text{Zn}(\text{NO}_3)_2 \cdot 6\text{H}_2\text{O}$  (297 mg, 1.0 mmol),  $\text{H}_2\text{L}^1$  (258 mg, 1.0 mmol), bibp (286 mg, 1.0 mmol), and water (8 mL) was placed in a 25-ml Teflon-lined stainless steel vessel. Subsequently the pH value was adjusted to 6.0 with 1 M NaOH solution, the mixture was heated at 160 °C for 3 d, and the reaction system was cooled to room temperature. Colorless crystals were obtained in yield 65% (based on Zn). Elemental analysis for  $\text{C}_{64}\text{H}_{44}\text{N}_8\text{O}_{10}\text{Zn}_2$ : calcd. C 63.22, H 3.65, N 9.22%; found C 63.25, H 3.63, N 9.28%. **FT-IR** (KBr, selected bands):  $\tilde{\nu} = 1596$  (s), 1548 (s), 1521 (s), 1386(s), 1235 (s), 1011 (s), 924 (s), 835 (s), 667 (m)  $\text{cm}^{-1}$ .

**Synthesis of 2:** A mixture of  $\text{CoCl}_2 \cdot 6\text{H}_2\text{O}$  (238 mg, 1.0 mmol),  $\text{H}_2\text{L}^2$  (350 mg, 1.0 mmol), bib (218 mg, 1.0 mmol), and water (8 mL) was placed in a 25-ml Teflon-lined stainless steel vessel. The pH value was adjusted to 6.0 with 1 M NaOH solution and the mixture was heated at 160 °C for 3 d. Afterwards the reaction system was cooled to room temperature. Purple crystals were obtained in yield 60% (based on Co). Elemental analysis for  $\text{C}_{30}\text{H}_{28}\text{CoN}_4\text{O}_8$ : calcd. C 57.06, H 4.47, N 8.87%; found C 57.11, H 4.40, N 8.82%. **FT-IR** (KBr, selected bands):  $\tilde{\nu} = 3421$  (s), 1610 (s), 1532 (m), 1387 (s), 1304 (s), 1248 (s), 1139 (s), 1067 (s), 1139 (s), 1067 (s), 933(m), 829 (m), 781 (s), 656 (s)  $\text{cm}^{-1}$ .

**Crystallographic Data Collection and Refinement:** Accurate unit cell parameters were determined by a least-squares fit of  $2\theta$  values, and intensity data were measured on a Rigaku with capital R area detector with  $\text{Mo-K}\alpha$  radiation ( $\lambda = 0.71073$ ) at room temperature. The intensities were corrected for Lorentz and polarization effects as well as for empirical absorption based on multi-scan technique. All structures were solved by direct methods and refined by full-matrix least-squares fitting on  $F^2$  by SHELX-97. All non-hydrogen atoms were refined with anisotropic thermal parameters. Crystallographic data for the compounds are summarized in Table 1 and selected bond lengths and angles are listed in Table 2.

**Table 1.** Crystallographic data and structure refinement details for 1 and 2.

	1	2
Formula	$\text{C}_{64}\text{H}_{44}\text{N}_8\text{O}_{10}\text{Zn}_2$	$\text{C}_{30}\text{H}_{28}\text{CoN}_4\text{O}_8$
Fw	1215.81	631.49
Crystal system	orthorhombic	triclinic
Space group	<i>Pnna</i>	<i>P</i> $\bar{1}$
<i>a</i> / Å	8.5510(17)	10.169(10)
<i>b</i> / Å	22.199(4)	11.891(9)
<i>c</i> / Å	14.867(3)	12.366(11)
<i>a</i> / °	90	92.341(15)
$\beta$ / °	90	112.077(19)
$\gamma$ / °	90	92.860(7)
<i>V</i> / Å <sup>3</sup>	2822.1(9)	1381(2)
<i>Z</i>	2	2
<i>D</i> / $\text{g}\cdot\text{cm}^{-3}$	1.431	1.519
<i>T</i> / K	293	293
<i>F</i> (000)	1248	654
Reflections collected / unique	24992 / 3237	14585 / 6480
GOF	1.034	1.075
$R_1, wR_2$ [ $I > 2\sigma$ ]	$R_1 = 0.0655$ $wR_2 = 0.1543$	$R_1 = 0.0335$ $wR_2 = 0.0815$

## Acknowledgements

This work was supported by the Natural Science Foundation of Shandong Province (ZR2010BQ033) and Science and Technology Basic Research Item of Qingdao City (12-1-4-2-(24)-jch).

**Table 2.** Selected bond lengths / Å and angles / ° for complexes 1 and 2.

1			
Zn(1)–O(1) <sup>#1</sup>	1.963(5)	Zn(1)–N(1) <sup>#1</sup>	2.011(3)
O(1) <sup>#1</sup> –Zn(1)–O(1)	99.1(3)	O(1) <sup>#1</sup> –Zn(1)–N(1)	132.5(2)
N(1)–Zn(1)–N(1) <sup>#1</sup>	99.3(2)		
2			
Co(1)–O(4) <sup>#2</sup>	1.9550(17)	Co(1)–O(2)	1.9574(17)
Co(1)–N(4)	2.035(2)	Co(1)–N(1) <sup>#3</sup>	2.049(2)
O(2)–Co(1)–N(4)	122.52(7)	O(4) <sup>#2</sup> –Co(1)–N(1) <sup>#3</sup>	119.48(8)
O(2)–Co(1)–N(1) <sup>#3</sup>	95.11(6)	N(4)–Co(1)–N(1) <sup>#3</sup>	101.42(6)
O(4) <sup>#2</sup> –Co(1)–N(4)	97.93(6)	O(4) <sup>#2</sup> –Co(1)–O(2)	120.38(7)

Symmetry transformations used to generate equivalent atoms: #1 *x*,  $-y+1/2$ ,  $-z+1/2$  for 1; #2  $-x+1$ ,  $-y+1$ ,  $-z+1$ , #3  $x+1$ , *y*,  $z+1$  for 2.

## References

- a) C. Janiak, *Angew. Chem. Int. Ed. Engl.* **1997**, *36*, 1431–1434; b) S. Noro, S. Kitagawa, M. Kondo, K. Seki, *Angew. Chem. Int. Ed.* **2000**, *39*, 2081–2084; c) M. J. Zaworotko, *Angew. Chem. Int. Ed.* **2000**, *39*, 2113–2116; d) R. Kitaura, K. Seki, G. Akiyama, S. Kitagawa, *Angew. Chem. Int. Ed.* **2003**, *42*, 428–431.
- a) M. Eddaoudi, H. Li, O. M. Yaghi, *J. Am. Chem. Soc.* **2000**, *122*, 1391–1397; b) C. J. Kepert, T. J. Prior, M. J. Rosseinsky, *J. Am. Chem. Soc.* **2001**, *123*, 10001–10011; c) S. Noro, R. Kitaura, M. Kondo, S. Kitagawa, T. Ishii, H. Matsuzaka, M. Yamashita, *J. Am. Chem. Soc.* **2002**, *124*, 2568–2583.
- a) S. R. Batten, R. Robson, *Angew. Chem. Int. Ed.* **1998**, *37*, 1460–1494; b) S. R. Batten, *CrystEngComm* **2001**, *3*, 67–73.
- a) L. Carlucci, G. Ciani, D. M. Proserpio, *Coord. Chem. Rev.* **2003**, *246*, 247–289; b) V. A. Blatov, L. Carlucci, G. Ciani, D. M. Proserpio, *CrystEngComm* **2004**, *6*, 377–395; c) I. A. Baburin, V. A. Blatov, L. Carlucci, G. Ciani, D. M. Proserpio, *J. Solid State Chem.* **2005**, *178*, 2452–2474.
- L. Carlucci, G. Ciani, D. M. Proserpio, *CrystEngComm* **2003**, *5*, 269–279.
- Y. Liu, Y. Qi, Y. Y. Lv, Y. X. Che, J. M. Zheng, *Cryst. Growth Des.* **2009**, *9*, 4797–4801.
- for examples: a) H. Wu, H. Y. Liu, B. Liu, J. Yang, Y. Y. Liu, J. F. Ma, Y. Y. Liu, H. Y. Bai, *CrystEngComm* **2011**, *13*, 3402–3407; b) H. Wu, H. Y. Liu, Y. Y. Liu, J. Yang, B. Liu, J. F. Ma, *Chem. Commun.* **2011**, *47*, 1818–1820; c) L. Carlucci, G. Ciani, M. Maggini, D. M. Proserpio, *Cryst. Growth Des.* **2008**, *8*, 162–165; d) P. Vishweshwar, D. A. Beauchamp, M. J. Zaworotko, *Cryst. Growth Des.* **2006**, *6*, 2429–2431; e) L. Carlucci, G. Ciani, D. M. Proserpio, *Chem. Commun.* **2004**, 380–381.
- a) Y. Q. Lan, S. L. Li, J. S. Qin, D. Y. Du, X. L. Wang, Z. M. Su, Q. Fu, *Inorg. Chem.* **2008**, *47*, 10600–10610; b) F. Luo, Y. T. Yang, Y. X. Che, J. M. Zheng, *CrystEngComm* **2008**, 981–982; c) J. Yang, J. F. Ma, S. R. Batten, Z. M. Su, *Chem. Commun.* **2008**, 2233–2234; d) G. H. Wang, Z. G. Li, H. Q. Jia, N. H. Hu, J. W. Xu, *Cryst. Growth Des.* **2008**, *8*, 1932–1939; e) C. Qin, X. L. Wang, E. B. Wang, Z. M. Su, *Inorg. Chem.* **2008**, *47*, 5555–5557.
- a) C. B. Aakeröy, N. R. Champness, C. Janiak, *CrystEngComm* **2010**, *12*, 22–43; b) H. A. Habib, J. Sanchiz, C. Janiak, *Inorg. Chim. Acta* **2009**, *362*, 2452–2460; c) H. A. Habib, A. Hoffmann, H. A. Höpfe, C. Janiak, *Dalton Trans.* **2009**, 1742–1751; d) H. A. Habib, J. Sanchiz, C. Janiak, *Dalton Trans.* **2008**, 1734–1744; e) B. Wisser, Y. Lu, C. Janiak, *Z. Anorg. Allg. Chem.* **2007**, *633*, 1189–1192.
- a) H. A. Habib, A. Hoffmann, H. A. Höpfe, G. Steinfeld, C. Janiak, *Inorg. Chem.* **2009**, *48*, 2166–2180; b) S. K. Henninger, H. A. Habib, C. Janiak, *J. Am. Chem. Soc.* **2009**, *131*, 2776–2777; c) B. Wisser, A. C. Chamayou, R. Miller, W. Scherer, C. Janiak, *CrystEngComm* **2008**, *10*, 461–464.
- Y. Qi, Y. X. Che, J. M. Zheng, *CrystEngComm* **2008**, *10*, 1137–1139.

- [12] V. A. Blatov, *TOPOS*, A Multipurpose Crystallochemical Analysis with the Program Package, Samara State University, Russia, **2004**.
- [13] a) The website of Reticular Chemistry Structure Resource (RCSR): <http://rcsr.anu.edu.au/>; b) S. S. Chen, Z. S. Bai, J. Fan, G. C. Lv, Z. Su, M. S. Chen, W. Y. Sun, *CrystEngComm* **2010**, *12*, 3091–3094; c) S. A. Bourne, J. J. Lu, B. Moulton, M. J. Zaworotko, *Chem. Commun.* **2001**, 861–862; d) A. S. R. Chesman, D. R. Turner, T. M. Ross, S. M. Neville, J. Z. Lu, K. S. Murray, S. R. Batten, *Polyhedron* **2010**, *29*, 2–9; e) F. Wang, X. H. Ke, J. B. Zhao, K. J. Deng, X. K. Leng, Z. F. Tian, L. L. Wen, D. F. Li, *Dalton Trans.* **2011**, *40*, 11856–11865.
- [14] Y. Qi, F. Luo, Y. X. Che, J. M. Zheng, *Cryst. Growth Des.* **2008**, *8*, 606–611.
- [15] Y. Wang, F. H. Zhao, Y. X. Che, J. M. Zheng, *Inorg. Chem. Commun.* **2012**, *15*, 180–183.

Received: May 9, 2013  
Published Online: July 16, 2013